

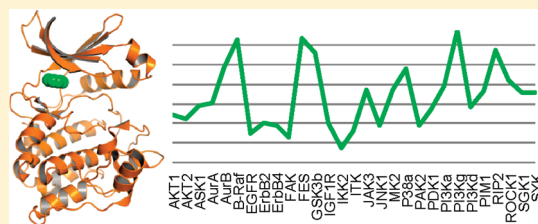
## Selectivity of Kinase Inhibitor Fragments

Paul Bamborough,\* Murray J. Brown, John A. Christopher,<sup>†</sup> Chun-wa Chung, and Geoff W. Mellor

GlaxoSmithKline R&amp;D, Medicines Research Centre, Gunnels Wood Road, Stevenage, Hertfordshire, SG1 2NY, U.K.

Supporting Information

**ABSTRACT:** A kinase-focused screening set of fragments has been assembled and has proved successful for the discovery of ligand-efficient hits against many targets. Here we present some of our general conclusions from this exercise. Notably, we present the first profiling results for literature fragments that have previously been used as starting points for optimization against individual kinases. We consider the importance of screening format and the extent to which selectivity is helpful in selecting fragments for progression. Results are also outlined for fragments targeting the DFG-out conformation and for atypical kinases such as PIM1 and lipid kinases.



## INTRODUCTION

Fragment-based drug discovery (FBDD) has received much attention as a strategy for the discovery of low molecular weight hits.<sup>1–4</sup> Many of these efforts have targeted protein kinases,<sup>5–15</sup> usually from the perspective of structure-based optimization against a single target. The selectivity of the fragments, and the extent to which this determines the selectivity of the compounds optimized from these hits, has received less attention.<sup>16,17</sup>

Whether inhibitors are optimized against a single target or simultaneously against several, tracking the selectivity profile is particularly important for kinase drug discovery.<sup>18–21</sup> Most inhibitors interact with the hinge motif within the ATP pocket, which is highly conserved between members of this family. Lack of appropriate selectivity is therefore a key obstacle to the development of compounds with a suitable therapeutic window. The main consideration is how and when the selectivity profile should be determined. Fragments are no different from other starting points in this respect, although it may be supposed that the smaller the inhibitor the more difficult it may be to achieve selectivity.<sup>17</sup>

Both diverse and target-focused fragment sets have been used as a source of starting points for optimization.<sup>9,22–24</sup> We have assembled a focused screening set of kinase-targeted fragments, aimed primarily though not exclusively at the ATP-binding pocket. In the process of ongoing screening, data have been accumulated that provide insights into the selectivity of fragments and an opportunity to draw some wider conclusions for FBDD and for kinase drug discovery. To our knowledge, this is the first detailed discussion of multikinase profiling of a set of fragment-sized compounds.

Here, we will consider the following questions:

- (1) Can biochemical assays be used for fragment screening? Are any assay formats less prone to interference than others?
- (2) Is a relatively small set of targeted fragments able to produce useful kinase hits?

- (3) Can hinge-binding fragments show kinase selectivity? Is it helpful to prioritize selective fragments for progression?
- (4) What are the selectivity profiles of non-ATP site fragments?
- (5) Are atypical kinases amenable to FBDD using a fragment set designed for typical ones?

## RESULTS

**Initial Validation.** Having constructed a focused kinase fragment set and checked its integrity (see Methods), its suitability as a source of kinase leads was assessed against one target,  $I\kappa B$  kinase  $\beta$  ( $IKK\beta$ ). The set was initially screened against  $IKK\beta$  in duplicate at a single compound concentration of 667  $\mu M$  using a TR-FRET based assay measuring the phosphorylation of the  $I\kappa B\alpha$  substrate. The reproducibility between replicates was excellent ( $r^2 = 0.93$ , Supporting Information, Figure S1).  $IC_{50}$  values were determined for active compounds, and a good relationship was found to exist between mean single-concentration and  $IC_{50}$  values. Known  $IKK\beta$  fragments were detected among the hits (Supporting Information, Figure S1).

Because of these encouraging results, the set was adopted as part of the standard lead discovery process for new kinase targets within GSK. In addition, the set was screened against key selectivity assays. Hits were confirmed first by  $IC_{50}$  determination and then by various methods depending pragmatically on the availability of follow-up screens for the kinase of interest. The set has delivered leads for multiple kinase targets, for example as reported recently for  $PDK1$ ,<sup>25</sup> and outcomes for other examples will be described elsewhere.

Here, we present results from the primary screens from a panel of 30 kinases (see Methods). We will first discuss the suitability of our assays as the primary step in FBDD.

Received: March 25, 2011

Published: June 23, 2011

**Assay Considerations.** It is recognized that assay interference can be problematic for some “traditional” biochemical formats. These may be sensitive to optical interference<sup>26</sup> and other non-specific artifacts<sup>27</sup> even at low micromolar compound screening concentrations. It is a concern that this may be more problematic at the higher concentration typically used for fragment screening. Consequently, while some have used biochemical assays as the primary fragment screen with success,<sup>28</sup> others favor the use of biophysical techniques such as NMR,<sup>5,6,29–31</sup> X-ray crystallography,<sup>7,32</sup> and SPR<sup>33–35</sup> as alternative technologies both to detect and to confirm target engagement of fragment hits.

Key to a successful fragment detection assay is high sensitivity, which results in a low false negative rate, coupled with high robustness and thus a low false positive rate. In these regards, NMR is often considered the “gold-standard” technique. NMR experiments can identify compounds with low % occupancy and confirm their structural integrity and aggregation state and can distinguish whether fragments are competitive with known ligands. However, the relatively high protein consumption, labor-intensive sample handling, and interpretation make NMR less ideal for larger compound libraries (>1–5K) and for subsequent SAR follow-up. One advantage that direct binding biophysical methods such as SPR and NMR retain over traditional activity or competition assays is that they are able to monitor binding to all sites on the protein target even when little is known about target activity. The corollary to this is that while binders can be found, their functional consequence may be poorly understood.

Several recent comparative studies using NMR data to define the “true” hits show that an optimized fragment set, rigorously validated for solubility and purity, can markedly reduce artifacts for both biophysical and biochemical assays.<sup>36,37</sup> The result is that both types of assay can be effective if sufficient care is taken to develop them for high concentration screening. The best results are obtained if orthogonal assays are used in series or parallel, be they purely biophysical, biochemical, or a combination. For kinases, the vast body of structural, chemical, and mechanistic information and an abundance of biochemical assay formats make biochemical assays a pragmatic choice for the first pass of a fragment screening cascade.

**Impact of Interference on Biochemical Assay Formats.** Given the perception that biochemical formats may be more prone to interference than biophysical ones, we have evaluated the possible influence of format-specific interference in our data set. Autofluorescence, inner filter effects, and insoluble particles leading to light scatter are common forms of optical interference that might be exacerbated by the high concentrations required for fragment screening (although this may be ameliorated by the smaller molecule size and higher solubility expected for fragments). The formats used in this analysis would show responses to optical interference (apparent inhibition or activation). Thus, we may predict that if optical interference is a significant issue for this fragment set, we might see greater than expected correlation between assays using the same format. The upper left half of Figure 1 depicts the correlation coefficient  $r^2$  between each pair of assay results. The correlation coefficients are generally quite low and are not skewed by outlying results (see Supporting Information Figure S2). Of course, it does not follow that high correlation must result from interference, especially between closely related kinases that tend to bind similar compounds.<sup>20,38,39</sup> For comparison, the pairwise sequence identity between kinase domains is indicated in the lower right half of Figure 1. We consider that the panel consists of kinases of sufficient diversity

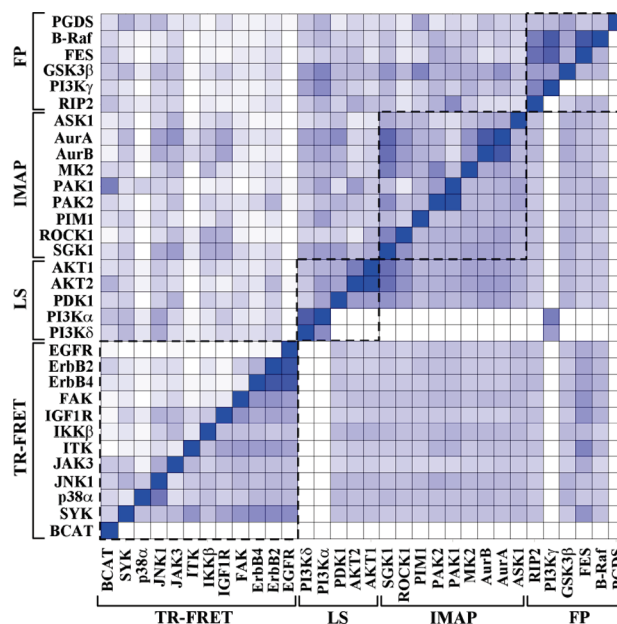


**Figure 1.** Correlation coefficients between all pairs of assays are shown in the upper left half ( $r^2$  between percentage inhibition values for all compounds). The color ranges from white ( $r^2 = 0$ ) to blue ( $r^2 = 1$ ). For comparison, the pairwise sequence identities over the kinase domain are shown in the lower right half. The dashed boxes mark assays of the same screening format. The greatest correlation is between the FP assays in the top-rightmost box.

that consistently low correlation between assays in one format with each other indicates a low incidence of format-dependent interference. We will now examine each format in turn to determine the susceptibility of each to interference.

In FP (fluorescence polarization) assays, compound autofluorescence gives apparent displacement, whereas light scatter from insoluble compounds appears as “activation”. Compound absorbance at the excitation or emission wavelengths should have no effect. In Figure 1, the FP assay results can be seen to be more highly correlated with each other than with the other assay formats. Five essentially unrelated kinases were screened in this format (B-Raf, FES, GSK3 $\beta$ , PI3K $\gamma$ , and RIP2). It seems unlikely that the correlation reflects structural similarity between these remotely homologous targets, so it is more likely due to interference. All five assays used fluorophores with similar excitation and emission wavelengths (rhodamine green or fluorescein). B-Raf, FES, and PI3K $\gamma$  used 1 nM fluoroligand (5 times lower than GSK3 $\beta$  and RIPK2) and show greater correlation of % inhibition. This may be because, assuming similar intrinsic brightness, assays running at lower fluoroligand concentration are more susceptible to interference through autofluorescence and light scatter. Even though the FP assays appear susceptible to these effects, this is still relatively uncommon: out of the 936 fragments, only 43 showed inhibition of >50% in all five FP format screens.

The IMAP (immobilized metal affinity phosphorylation) format<sup>40</sup> is less susceptible to interference than the FP binding assays despite the same polarization end-point, due to the higher concentration of fluorophore used. LEADseeker assays<sup>41</sup> are affected by compound absorbance (color quench), but the long wavelengths mean it is unlikely to see interference from fragments. It was to be expected that these assays would show a lower internal correlation than FP, and this was found to be the

**Table 1.** Mean Percentage Inhibition Profiles of Fragments 1–17 at Compound Concentrations Listed in Supporting Information Figure S3<sup>a</sup>

	1	2	3	4	5	6	7	8	9	10	11	12	13	14	15	16	17
AKT1	20	21	48	24	29	19	19	10	67	17	9	19	6	0	11	0	17
AKT2	7	16	19	12	25	16	14	13	39	8	12	15	0	6	16	9	9
ASK1	88	10	42	31	39	80	52	17	77	1	13	3	9	0	8	9	2
AurA	90	89	36	37	40	84	92	27	96	0	7	27	7	17	0	5	0
AurB	99	97	94	81	77	98	100	22	97	0	0	31	12	12	30	15	6
B-Raf	63	10	19	0	100	20	26	17	55	59	67	71	33	17	8	12	6
EGFR	11	0	0	0	9	0	18	25	36	8	0	4	0	4	0	5	5
ErbB2	3	4	0	0	21	1	9	0	25	0	2	0	0	0	2	5	0
ErbB4	9	15	5	5	17	0	13	0	47	0	0	0	0	0	0	0	44
FAK	5	10	3	3	6	13	7	1	33	0	6	3	4	6	30	6	0
FES	20	35	9	1	100	11	12	14	68	70	3	3	0	6	13	1	9
GSK3 $\beta$	57	55	21	35	92	34	59	41	66	19	34	19	22	19	11	23	13
IGF1R	44	18	23	24	20	47	15	92	0	5	0	0	1	6	0	0	0
IKK $\beta$	22	8	29	15	0	47	65	0	57	0	3	2	0	0	0	0	0
ITK	87	69	44	26	12	41	39	24	94	6	30	0	0	0	0	14	41
JAK3	78	36	53	29	54	72	54	5	74	0	0	0	0	0	0	0	2
JNK1	33	74	15	13	18	34	20	13	83	14	2	4	0	0	0	16	1
MK2	80	24	42	42	54	54	47	24	28	0	24	28	13	16	18	8	7
P38 $\alpha$	24	34	0	14	76	8	14	13	61	42	99	96	64	79	53	42	25
PAK1	19	12	17	0	38	0	14	0	0	0	0	0	0	0	0	0	14
PAK2	36	3	4	5	17	16	7	3	32	0	0	0	0	5	5	2	4
PDK1	77	27	25	25	35	53	40	17	66	2	15	25	15	8	20	11	9
PI3K $\alpha$	45	14	16	6	59	22	29	24	86	46	27	40	4	10	11	16	20
PI3K $\delta$	68	19	22	10	36	19	18	16	90	42	27	41	8	10	11	10	7
PI3K $\gamma$	66	16	20	0	100	10	20	13	70	92	2	9	0	7	9	13	2
PIM1	20	6	6	22	54	21	21	5	89	39	1	19	13	10	12	58	17
RIP2	11	24	5	0	94	11	10	2	69	0	0	7	1	0	0	7	6
ROCK1	80	10	76	80	64	65	46	25	93	0	6	9	7	8	5	3	0
SGK1	76	21	62	75	52	97	63	27	90	0	7	10	8	8	15	17	3
SYK	56	94	27	21	51	25	36	26	86	15	3	20	0	0	87	6	8

<sup>a</sup>In this table only, apparent % inhibition values of >100% have been rounded to 100; those of <0% are indicated as 0.

case (Figure 1). Of the 936 fragments, 14 compounds inhibited all nine IMAP assays by >50%, and 11 inhibited all five LEADseeker assays by >50%. However, these values are influenced by the inclusion of closely homologous kinases in the screening panel, which would be expected to bind similar compounds. This is especially obvious in Figure 1 for the most closely related pairs, AurA/AurB and PI3K $\alpha$ /PI3K $\delta$ .

TR-FRET (time-resolved fluorescence resonance energy transfer) assays are resilient to interference from compound autofluorescence because of the time-resolved nature of the readout (compound autofluorescence is usually prompt). Inner filter effects (absorbance) can be minimized by taking into account effects on the donor and acceptor emission. The main interference comes from compound insolubility that usually appears as apparent activation. As expected for a set of small fragments with relatively high solubility, the TR-FRET format output is only weakly correlated between kinases (Figure 1), suggesting that artifacts in these assays are relatively rare.

The set was also screened against two non-kinases as selectivity assays:  $\beta$ -catenin in TR-FRET format and prostaglandin-D synthase (PGDS) in FP format. The greatest correlation between results from the  $\beta$ -catenin assay and any kinase was with the PAK1

IMAP assay ( $r^2 = 0.48$ ). The reason for this is unclear because the next highest correlation was with the AKT2 LEADseeker assay ( $r^2 = 0.31$ ). Results from the PGDS FP assay only weakly correlated with results from any kinase, although the greatest correlation was with the FP assays (e.g., GSK3 $\beta$ ,  $r^2 = 0.37$ ).

The correlation between screens was generally low, suggesting that the incidence of interference due to the biochemical assay format was low as a proportion of compounds tested. This finding suggests that the assay formats are all suitable for use as the first stage of a fragment screen and that our subsequent analysis of selectivity profiles using this data is valid. Nevertheless, the FP format appears more prone to false positives than the others, so they are probably better avoided for fragment screening if a TR-FRET assay is available. Whichever format is used, the results should still be treated with caution and confirmed by other means. The incidence of putative false positives was not so high that it would prevent hit triage using another assay, such as the type of counterscreen for interference often employed in micromolar-concentration screening<sup>27</sup> or the biophysical methods frequently used in fragment-based lead discovery. For example, to follow up the PDK1 LEADseeker hits, 18 fragments were tested in an NMR screen. Only five showed no sign of interaction.<sup>25</sup>

**Kinase Selectivity Profiles.** We will now turn to the profiles of kinase fragments, beginning with a detailed discussion of five (1–5) from the literature (Table 1, Figure 2). The optimization of these starting points has been reported, but little information was disclosed about their inhibition profiles. Figure 3 illustrates the range of different profiles that can be obtained even from these simple hinge-binding fragments.

**Profiles of Literature Kinase Inhibitor Fragments.** (1) *Adenine*. Even adenine (1) shows distinctly different inhibition of different kinases (Figure 3, black line). Adenine significantly inhibited the activity of kinases including ASK1, AurA, ITK, JAK3, and ROCK1. Unexpectedly, it showed little inhibition of EGFR, ErbB2, ErbB4, FAK, and RIP2 kinases. Given that this is the hinge-binding fragment of ATP, it is unsurprising that other fragments also exhibit distinct profiles.

(2) *2-Anilinoypyrimidine*. 2-Anilinoypyrimidines are among the most commonly recurring templates in kinase inhibitor medicinal chemistry. Despite this, fragment 2 strongly inhibited only six kinases: Aurora A/B, GSK3 $\beta$ , ITK, JNK1, and SYK (Figure 3, red line). A literature search identified compounds containing this fragment as a hinge-binding motif that also have activity against these targets. Some examples are 2a–c (Figure 4).<sup>42–44</sup>

Surprisingly, 2 is only a very weak inhibitor of other kinases that it might have been expected to inhibit more potently. For example, potent and selective inhibitors of IKK $\beta$  and p38 $\alpha$  such as 2d and 2e utilize the fragment as their hinge-binding motif. These have nanomolar-range potency against their respective targets<sup>45,46</sup> with ligand efficiencies  $LE \approx (-RT \ln IC_{50}) / (\text{number of heavy atoms})^{47}$  based upon literature  $IC_{50}$  of 0.38 and 0.34. However, when our fragments are ranked against IKK $\beta$  and p38 $\alpha$ , either by % inhibition or by a ligand efficiency metric (% I per heavy atom), 2 is found well down the list (Table 2). Had hits been chosen to progress against these targets from this fragment set based on ligand efficiency alone, it is unlikely that fragment 2 would have been among them.

(3) *7-Azaindoles*. 7-Azaindoles 3 has been reported as an inhibitor of AKT2, CDK5, and GSK3.<sup>48–50</sup> In our assays it was only a weak GSK3 $\beta$  inhibitor, but it efficiently inhibited AurB, ROCK1, and SGK1 (Table 1; Figure 3, green line). It also inhibited numerous other kinases at a lower but significant level,

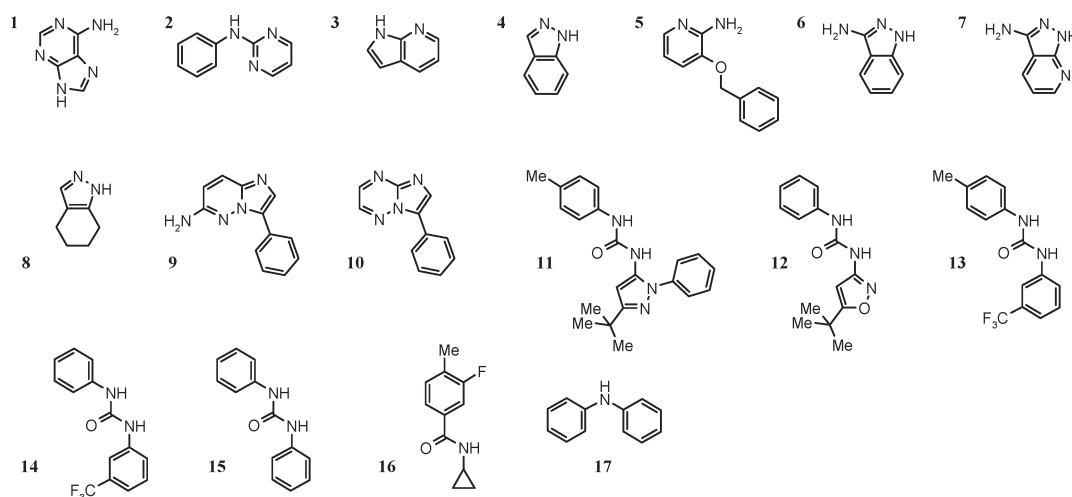


Figure 2. Kinase inhibitor fragment structures.

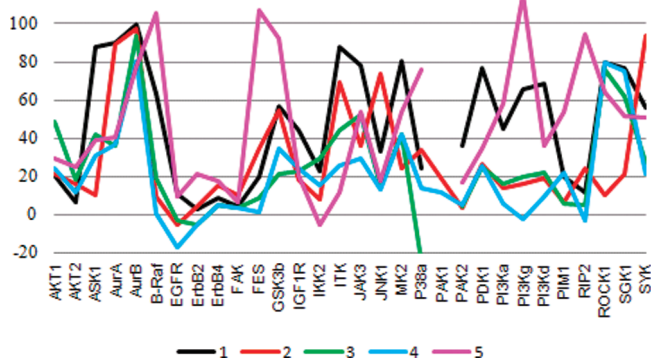


Figure 3. The % inhibition profiles of fragments 1–5 (in assay formats listed in Supporting Information Figure S3).

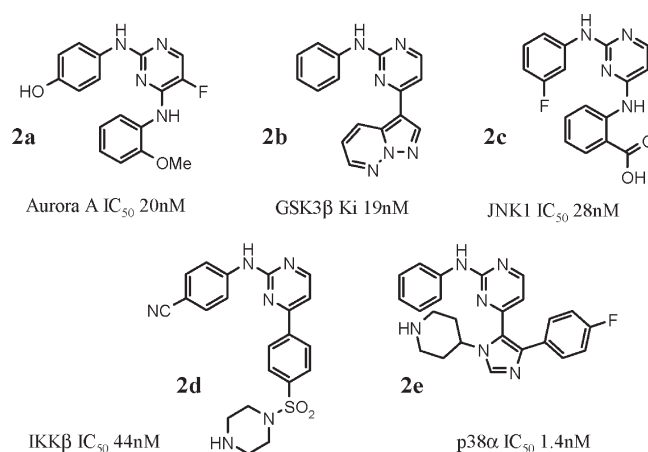


Figure 4. 2-Anilino-1H-pyrimidine containing inhibitors.<sup>42–46</sup>

including IKK $\beta$ , JAK3, and AKT1. Compounds containing 7-azaindole hinge-binding groups have been reported as inhibitors of many of these kinases, notably AKT (3a, Figure 5)<sup>51</sup> and SGK1 (3b).<sup>52</sup> Encouragingly, 3 ranked 15th out of our hits against AKT1 when ranked by efficiency (Table 2).

As with 2-anilino-1H-pyrimidine 2, the 7-azaindole fragment 3 only weakly inhibited some kinases that it might have been expected to inhibit more strongly. For example, 3c and 3d are potent inhibitors of IKK $\beta$ <sup>53</sup> and the JNKs,<sup>54</sup> respectively, with LEs (based upon literature IC<sub>50</sub>) of 0.45 and >0.42. However, when the fragment set is ranked by % inhibition of IKK $\beta$  or JNK1 or % I per heavy atom, 3 ranks relatively low down the list (Table 2).

(4) 2-Azaindoles (Indazoles). 2-Azaindole (4) has been reported as a CDK2 inhibitor with IC<sub>50</sub> of 185  $\mu$ M and has featured as a FBDD starting point for that target.<sup>55</sup> CDK2 was not present in our panel, but 4 also efficiently inhibited AurB, ROCK1, and SGK1 (Table 1; Figure 3, blue line). This hinge-binding fragment was also used to develop potent AKT inhibitors,<sup>56</sup> although 4 was not especially potent in our assays or highly ranked by efficiency against AKT1 (Table 2).

Surprisingly, the 2- and 7-azaindoles 3 and 4 show strikingly similar kinase inhibition profiles (Figure 3, green and blue). Both bind potently to Aurora B, ROCK1, and SGK1. It is possible that these kinases respond especially well to very small fragments that

occupy only the hinge-binding region (3 and 4 are among the smallest in the set). This might be characteristic of AGC family kinases, which have more lipophilic ATP pockets that are partially occupied by a conserved phenylalanine side chain from the C-terminal extension to the kinase domain. Other kinases that do not bind well to such small fragments may require additional interactions for potent inhibition.

The above examples highlight the success of our focused fragment set in finding active, ligand-efficient fragments against multiple kinases. Other examples included many that are more efficient than precedented hinge-binding fragments featuring in optimized, potent, and efficient literature inhibitors. This success led to a different problem, namely that the numerous hits must somehow be prioritized for progression. One way to do this would be to use ligand efficiency as a ranking tool. However, as we have shown above (e.g., 2 for p38 $\alpha$ , 3 for IKK $\beta$ , or 4 for AKT1), potentially valuable hits that could be optimized to very acceptable compounds with little loss of LE appear some way down the list of hinge-binding fragments.

Relationships between fragments and leads have been explored before while focusing on contributions to binding energy, by decomposing potent inhibitors into their constituent parts.<sup>57</sup>

**Table 2. Estimated Maximum Ligand Efficiencies of 2–4 against Kinases Known To Bind Elaborated Analogues Efficiently**

compd	kinase	%I <sup>a</sup>	r%I <sup>b</sup>	rEff <sup>c</sup>	IC <sub>50</sub> <sup>d</sup>	pIC <sub>50</sub> <sup>e</sup>	LE <sup>f</sup>
2	p38α	34	302	280	>667	<3.2	<0.34
2	IKKβ	8	226	242	>667	<3.2	<0.34
3	AKT1	48	61	15	>400	<3.4	<0.53
3	IKKβ	29	97	71	>667	<3.2	<0.50
3	JNK1	16	445	335	>667	<3.2	<0.50
4	AKT1	24	249	127	>400	<3.4	<0.53

<sup>a</sup>Percent inhibition. <sup>b</sup>Rank by %I out of 936 fragments. <sup>c</sup>Rank by efficiency, %I/(number heavy atoms). <sup>d</sup>A very approximate estimate of the minimum IC<sub>50</sub> (for compounds with <50% inhibition, this is the screening concentration in μM). <sup>e</sup>Max pIC<sub>50</sub>. <sup>f</sup>Maximum LE (1.37 × pIC<sub>50</sub>)/number heavy atoms).

The study found a roughly linear relationship between molecular size and the maximum binding energy obtainable within a series, the gradient of which varied somewhat from target to target. It does not follow that all starting points are equally amenable to be optimized, as the slope may also vary from series to series. For example, a highly efficient fragment may lack a substitution point permitting elaboration into a pocket that a less efficient fragment can grow into. Alternatively, elaboration of an efficient fragment at a given position might be tolerated only at the expense of compromises, producing nonadditivity of fragment binding energy such that the whole is less than the sum of its parts. Such compromises might include changes to the binding mode of the fragment in its elaborated context.<sup>58</sup> Modifications resulting in unfavorable conformational changes in the protein or more subtle factors such as altered solvent interactions in the bound complex or in solution would produce the same effect.

Another potential problem with relying on LE to choose fragments for progression stems from the conservation of the kinase ATP site around the hinge. Inhibitors that rely on tight interactions with this region might have reduced opportunities for selectivity, in which case the most efficient fragments may not always be the best to take forward into optimization. Other considerations (for instance, predicted developability characteristics, undesirable chemical functionality, intellectual property considerations, etc.) may also count against the most efficient hits. While some of these factors may be predictable from the fragment alone, others such as high clearance or low bioavailability may only manifest themselves in later compounds during optimization. We also note that the fragments with the greatest apparent efficiency seem most likely to be biochemical assay artifacts. For example, in our recent PDK1 example 5 out of 18 compounds showed no trace of interaction by NMR saturation transfer difference. Four out of these five were among the six most efficient fragments found.<sup>25</sup>

It is tempting to consider alternative ways to prioritize fragment hits. For example, their selectivity profiles could be generated and the most selective hits prioritized. The next example shows that this strategy could also be problematic if rigorously applied.

(5) *Benzoyloxy pyridine*. Fragment 5 was a 1.3 mM fragment hit used in a successful case study of structure-based optimization for p38α.<sup>8</sup> In our hands it also inhibited Aurora A/B, FES, GSK3β, JAK3, MK2, PI3Kγ, and RIP2 to a similar extent (Table 1; Figure 3, magenta line). Clearly, the fragment has a complex profile, yet the compounds derived from 5 were selective p38α

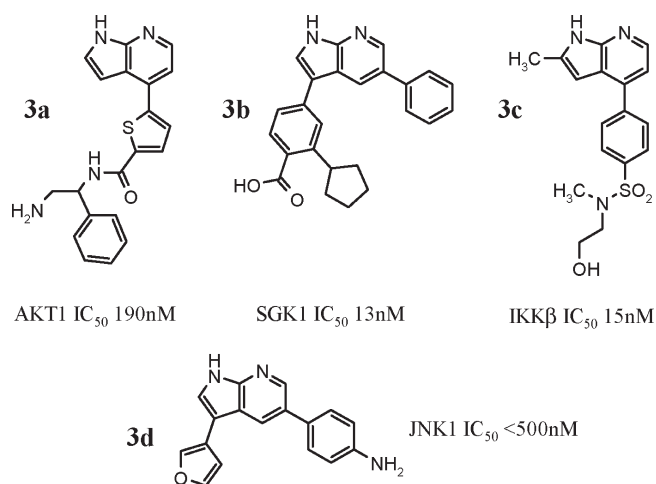


**Figure 5.** 7-Azaindole containing inhibitors 3a–d.<sup>51–54</sup>

inhibitors. The selectivity was introduced by elaboration of the template (in this case, by growing from the ATP pocket into the DFG-out pocket).

This example argues against overinterpretation of the selectivity of fragments at too early a stage. Selectivity, like potency, is context-dependent and can change greatly during modification. Next, we will discuss the extent to which this is generally the case.

#### Do Selective Fragments Produce Selective Compounds?

We sought to answer the above question by comparing the hit rates of our fragments to larger molecules containing those fragments. This is not an easy exercise, as few lead-sized kinase inhibitors have been screened against the same kinase panel as our fragments. We opted to use a data set of 577 leadlike compounds screened against 203 kinases,<sup>20</sup> almost 80% of which had molecular weight under 400.

The fragments were subjected to a cleaning procedure to strip from them substituents judged to be unfunctional (see Methods). The lead-sized compounds were then analyzed and the presence of each of the fragment substructures marked. This produced a list of 592 matched pairs of lead-sized compounds and their associated fragment substructures. For the majority of these pairs, the fragment corresponds to the probable hinge-binding group of the elaborated molecule. The selectivity of fragments and their associated elaborated partners was quantified using a selectivity index (*S*) analogous to that of Karaman et al.<sup>59</sup> (Figure 6).

While some fragments inhibit numerous kinases (high *S*), many are surprisingly selective. In general, though, the fragments do have higher *S* (are less selective) than the elaborated compounds. This is as would be expected following the reduced complexity argument of Hann et al.<sup>1</sup> However, it is difficult to conclude from this analysis that fragments are less selective than larger molecules, since the panels have different kinase compositions and the choices of activity thresholds are subjective.

There is no correlation between the hit rates of the fragments and those of their elaborated partners. Intuitively, it seems sensible to choose selective fragments for optimization over unselective ones, all else being equal, in the hope that this selectivity will be maintained. However, our data suggest that it is not uncommon to find selective lead-sized compounds based upon unselective fragments (Figure 6, upper left). Equally, unselective leadlike compounds are frequently based upon selective fragments (Figure 6,

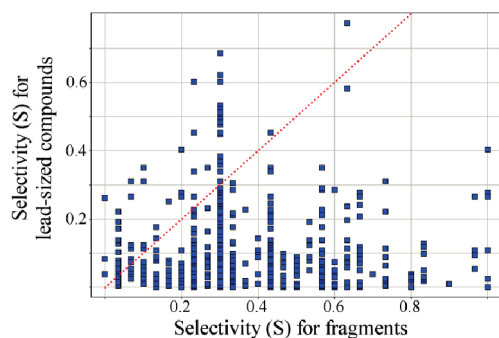


**Figure 6.** Selectivity index ( $S$ ) of fragments (fraction of the 30 kinases inhibited by 30% or more) vs selectivity index of their associated lead-sized molecules (fraction of the 203 kinases bound with % control of <10). This is depicted as a box plot in Supporting Information Figure S4.

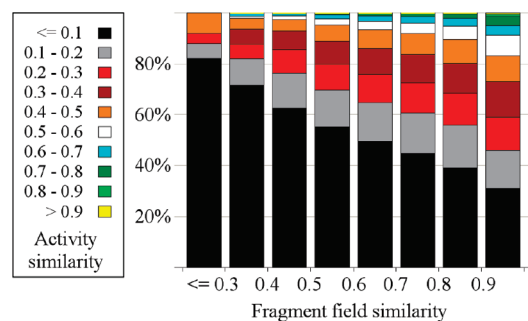
lower right). It seems that the property of selectivity need not be maintained between fragments and their related lead-sized molecules. This is not an unexpected result, given the earlier discussion of the possible causes of nonadditivity in binding energy for a single target, especially since the differences between kinases tend to become more pronounced moving away from the hinge region.

Another caveat of this analysis is that the lead-sized molecules were not produced by optimization of the fragments. Such a data set would be preferable but is not currently available. The influence of rational design during fragment elaboration may greatly influence the selectivity outcome. Our results emphasize that, at very least, careful selection of substituents would be needed to preserve the selectivity profile of a fragment during optimization. We will now conclude our discussion of hinge-binding fragments by examining the relationship between selectivity profile and structure.

**Origins of Fragment Selectivity.** Fragments must exploit very subtle differences between ATP-binding sites in order to obtain their selectivity profiles. If fragments with similar profiles exploit similar recognition features, then fragments with similar 3D structures should have similar inhibition profiles.

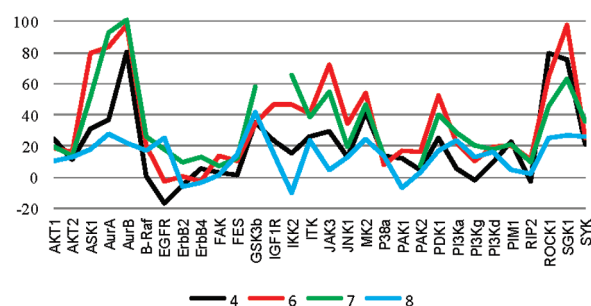
Considering each possible pair of fragments within the set, two similarity values were calculated (see Methods). The first (*activity similarity*) represents the similarity between their activity profiles. The second (*field similarity*) is a score in which the 3D structures of the fragments are overlaid while attempting to maximize the similarity between their field points. The resulting score aims to represent the similarity between ligands from the point of view of the receptor. As an illustration, similarity scores between compounds 1–17 are given in Supporting Information Figure S5.

Figure 7 shows the relationship between activity similarity and field similarity over all pairs of fragments. Dissimilar fragments (left-hand side, field similarity of  $\leq 0.3$ ) usually have different inhibition profiles. The activity similarity increases toward the right with increasing field similarity. This relationship is exactly as would be expected, but it is reassuring that it is observed and that the interaction fields can discriminate between such small fragments. Virtual screening using interaction fields could be a useful way to find novel fragments with similar profiles to known starting points. The field approach has been used before to identify kinase inhibitors<sup>60</sup> but is complicated by the need to consider multiple conformers of each compound. Since small molecules can adopt few distinct conformers, this approach would be particularly well suited to fragments.



**Figure 7.** Dependence of fragment inhibition profile on field similarity for pairs of fragments.

a)



b)

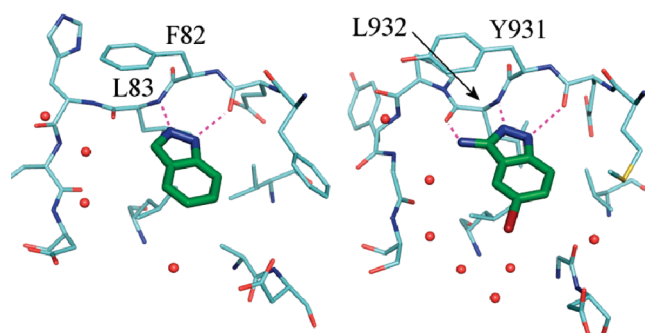


**Figure 8.** (a) Profiles of 4, 6, 7, and 8. (b) Left: X-ray structure of CDK2 with bound 2-azaindole.<sup>55</sup> Right: X-ray structure of JAK2 with bound 3-amino 5-bromo 2-azaindole.<sup>61</sup> Hydrogen bonds are shown as magenta dotted lines.

As apparent from Figure 7, a minority of fragment pairs with high field similarity scores have dissimilar activity profiles. We examined extreme outliers from the fragment set (fragments with high field similarity, yet different inhibition profiles) to see if these could be explained.

**Fragments with High Field Similarity.** The 2-azaindole 4 and 6–8 are examples of fragments with high field similarity to one another (Supporting Information, Figure S5). Unsurprisingly, 6 and 7 have profiles similar to one another (Figure 8a, red and green lines). The profile of fragment 4 is also broadly similar, but it shows weaker inhibition of most kinases (Figure 8a, black line). This illustrates the increased activity arising from the addition of a simple amino group, which can be interpreted as the formation of an additional hydrogen bond to the hinge. This can be visualized by comparing the crystal structure of 4 bound to

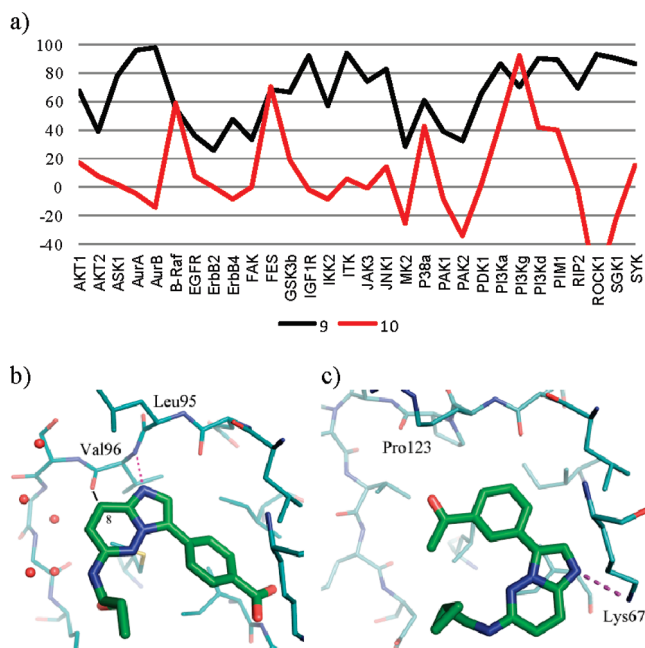


**Figure 9.** (a) Profiles of **9** and **10**. (b) Crystal structure of DAPK3 with a bound imidazopyridazine.<sup>62</sup> The single hydrogen bond to the hinge (magenta dotted line) and the 3.1 Å contact between the 8-position and the Val96 carbonyl (black solid line) are shown. (c) Crystal structure of PIM1 with a bound imidazopyridazine.<sup>64</sup>

CDK2<sup>55</sup> to that of a bromine analogue of **6** bound to JAK2<sup>61</sup> (Figure 8b). Interestingly, even though this part of the hinge is similar in most protein kinases, the SAR suggests that this interaction is subtle and is more important for some kinases than others.

Another similar fragment, **8**, is of comparable size to **4** but generally much weaker (Figure 8a, blue). This reflects the preference for aromaticity rather than an aliphatic ring within the adenine pocket of all kinases in the panel.

Fragments **9** and **10** are another interesting pair of fragments with high field similarity. Elaborated compounds containing the imidazopyridazine fragment **9** have been found active against several kinases, notably DAPK3. In contrast, the imidazotriazine **10** shows weaker inhibition of most kinases tested in our panel (Figure 9a). This can be rationalized by referring to the crystal structure of an elaborated imidazopyridazine in DAPK3<sup>62</sup> (Figure 9b). If the carbon at the 8-position of the imidazo[1,2-*b*]pyridazine core were replaced by nitrogen in this binding mode, the nitrogen would lie within 3.1 Å of the outer-hinge carbonyl oxygen of Val96, an unfavorable electrostatic interaction. This backbone carbonyl is spatially conserved across multiple protein kinases, explaining the general trend for lower activity of fragment **10**. There are a few exceptions for which **9** and **10** show similar activity. There is no obvious explanation for this in B-Raf and FES, but it can be rationalized for p38 $\alpha$ , as it is known that the presence of a glycine residue proximal to the hinge region (Gly110) can allow sufficient flexibility for the carbonyl to rotate to point away from inhibitors of this kinase.<sup>63</sup> The PI3 kinases also differ from most protein kinases in the space available to ligands around this region of the hinge.

To conclude this section, fragments have distinct inhibition profiles that are related to their 3D features so that similar fragments tend to show similar kinase profiles. When they do not, the reason for the discrepancy can often be rationalized by

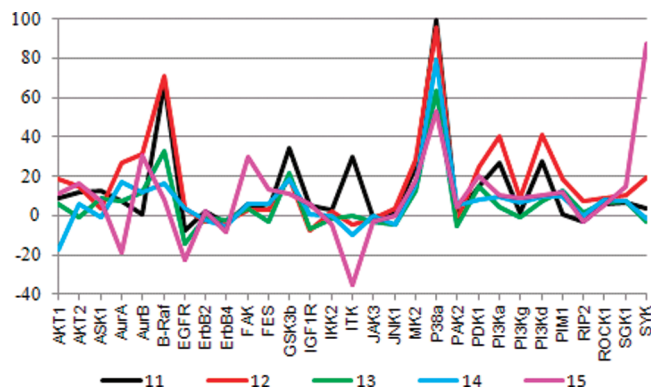


**Figure 10.** Profiles of biarylureas **11–15**.

structure-based modeling. This adds further weight to the interpretation of the single-concentration screening results and also suggests that field similarity is one valid virtual screening approach to discover new fragment inhibitors with kinase profiles similar to that of a known fragment. However, as discussed above, it is not necessarily the case that such a fragment can be optimized without altering its selectivity profile.

All of the discussion to this point has concentrated on fragments that target the hinge region of the ATP site. We will now briefly discuss our results for fragments intended to bind elsewhere.

**Fragments beyond the ATP Site.** Published examples of kinase FBDD have tended to concentrate on ATP-site fragments, as does our targeted fragment set. Binding of small molecules away from the hinge has been reported,<sup>65</sup> although usually with lower efficiency than hinge-binding fragments, and without reporting cross-kinase profile data. To learn more about fragments binding away from the ATP site, several compounds thought likely to do this were included in the set.

**DFG-Out Fragments.** The first report of a fragment conclusively shown to bind outside the ATP pocket of a kinase domain with submicromolar affinity was a biarylurea binding to the DFG-out pocket of p38 $\alpha$ .<sup>66</sup> The DFG-out conformation, involving a rearrangement of the DFG motif, has been seen in inhibitor-bound X-ray complexes with several kinases other than p38 $\alpha$ , mainly tyrosine kinases (e.g., c-Abl<sup>67</sup> and B-Raf<sup>68</sup>). Many have suggested that targeting this pocket should increase the selectivity of inhibitors for these kinases.

Biarylureas or biaryl amides are the simplest known substructures able to take advantage of the DFG-out conformation of a number of kinases. The selectivity profiles of such fragments containing the DFG-out pharmacophore have not been reported. We therefore included a number of biarylureas (**11–15**) in the compound set. The results are shown in Table 1 and Figure 10. The apparent activity of **15** against SYK was unexpected, since this kinase has not been reported to bind compounds in a DFG-out mode, so **15** was retested in dose–response mode. The high % I activity was not reproduced ( $IC_{50} > 660 \mu M$ , 1 of only 4 out of 58 compounds showing >80% I against SYK that failed to give a fitted dose–response curve).

As expected, the biarylureas with a 3-substituted aryl ring (**11–14**) inhibited p38 $\alpha$  and B-Raf. The unsubstituted urea **15** had the lowest p38 $\alpha$  activity (Figure 10), consistent with SAR from elaborated analogues, which require the occupation of a lipophilic pocket within the DFG-out pocket by a substituent at the 3-aryl position for potency.<sup>69,70</sup> In general, other than those

mentioned above, most kinases tested showed little consistent evidence of inhibition by DFG-out fragments (Figure 10). There are several possible interpretations of this result. Different chemotypes may be needed to stabilize the DFG-out conformation of these kinases. The biarylamide or biarylurea motif interacts with all kinases to which they have been seen to bind crystallographically through structurally conserved catalytic residues, but we note that the first reported PDK1 and IGF-1R DFG-out binding inhibitors have quite different chemical motifs.<sup>15,71,72</sup> Alternatively, the ability to adopt a low-energy DFG-out conformation may be limited to a subset of kinases. In some tyrosine kinases, mutation of wild-type threonine gatekeeper residues to larger amino acids may destabilize the DFG-out conformation.<sup>73</sup> Consistent with this, out of the kinases in our panel apart from p38 $\alpha$  and B-Raf, only RIP2 and the three members of the Erb family have threonine gatekeepers, while all of the rest are larger. Another possibility is that this conformation may not be accessible to some of the active kinases used in these biochemical assays, but activity-based screens have frequently been used to detect DFG-out inhibitors of various kinases.<sup>70,74–79</sup> Whatever the reason, these data suggest that for most kinases in this panel the development of DFG-out inhibitors may be challenging.

**Other Nonhinge Binding Fragments.** Compounds binding primarily in the ATP site can gain considerable affinity and specificity from interactions in neighboring pockets. An example from our own p38 $\alpha$  work is the cyclopropylamide **16**, which binds into the back pocket and to the DFG motif catalytic residues without inducing the DFG-out conformation. Elaborated compounds containing the cyclopropylamide fragment were weaker than analogues containing a DFG-out pharmacophore but were more ligand-efficient and more selective.<sup>70</sup> Consistent with this, the fragment showed inhibition of p38 $\alpha$  (Table 1) but was weaker than the DFG-out fragments **11–14**, and binding of **16** to most other kinases was minimal.

Another nonhinge binding fragment included in this set was the aniline **17**. This was included on the basis of observations that bis-aryl anilines are frequently present in ATP-site kinase inhibitors.<sup>80</sup> Even when lacking the hinge-binding hydrogen bond acceptor functionality, anilines frequently bind in lipophilic kinase pockets. For most kinases tested, this simple lipophilic fragment was too weak to show convincing inhibition (Table 1). While it did show reproducible inhibition of two kinases, ErbB4 and ITK, the activity is low compared to the hinge-binding fragments tested.

Finally, we will turn our attention to some of the atypical kinases in our screening panel. We aimed to determine whether inhibitors of these would be found within a fragment set targeting the ATP site interactions of typical protein kinases.

**Atypical Kinase 1: PIM1.** Numerous hits from the fragment set were found that inhibit PIM1. This is surprising, since PIM1 is an atypical kinase with a proline hinge residue, rendering it incapable of forming the canonical ATP-site hydrogen bond interaction used as the basis for the design of the compound set.<sup>64</sup> In general, fragments that inhibited PIM1 frequently inhibited other protein kinases. Out of 115 compounds showing  $\geq 80\%$  PIM1 inhibition, 89 inhibited at least one other protein kinase at the same threshold. To exclude the possibility of assay interference, because PIM1 was screened as an IMAP assay, we examined the frequency with which these compounds were active in the 11 TR-FRET assays (which as shown earlier have little correlation with the IMAP format). Fifty-two compounds exhibited  $\geq 80\%$  inhibition of at least one of these other kinases.

It has been noted before that groups that might be expected to bind to the hinge of a typical kinase can bind to the opposite side of the ATP-binding site of PIM1, through hydrogen bonds to the conserved catalytic residues K67 and E89 and associated water molecules. A very recent publication reported the identification of fragments related to cinnamic acid that make the same interaction via a carboxylate.<sup>81</sup> The hydrogen-bonding and steric requirements for a ligand to bind in this way are similar to those required for a conventional hinge-binding motif. This has been seen crystallographically with the imidazopyridazine template, which binds in different modes to PIM1 and to DAPK3<sup>62,64</sup> (Figure 9b and Figure 9c). Our results suggest that it might be very common for conventional hinge-binding fragments to interact with the catalytic region of PIM1.

**Atypical Kinase 2: Lipid Kinases.** The kinase panel contained three lipid kinases, the PI3K $\alpha$ ,  $\gamma$ , and  $\delta$  isoforms, that had not been the subject of FBDD before. While this manuscript was in preparation, the first report of the discovery of PI3K fragments was published.<sup>82</sup> This study used a molecular docking approach to select fragments for test against a panel of four PI3 kinase AlphaLISA assays. A detailed discussion of our PI3K results is beyond the scope of this manuscript. However, we note the following:

- (1) There was a high hit-rate against all three PI3Ks (Supporting Information Figure S3). 156 fragments inhibited both  $\alpha$  and  $\delta$  isoforms with 50% or greater inhibition.
- (2) The results from the PI3K $\alpha$  assay correlated closely with those from the PI3K $\delta$  assay ( $r^2 = 0.70$ , Figure 1), consistent with their close homology. 156 fragments inhibited both isoforms with  $>50\%$  I. The correlation between these isoforms and PI3K $\gamma$  was lower ( $r^2 = 0.47$  and  $0.39$ , Supporting Information Figure S2), but these values are still greater than the correlation coefficient between PI3K $\gamma$  and any other kinase, apart from the others screened in the FP format.
- (3) There was a high incidence of crossover between PI3K activity and activity against protein kinases. 154 of the 156 fragments that inhibited PI3K $\alpha$  and PI3K $\delta$  with  $>50\%$  inhibition also inhibited at least one protein kinase by 50% or more. This number dropped to 152 when the FP assays were excluded and to 128 when only the 11 TR-FRET assays (with the lowest potential interference rate) were considered.

We conclude that despite the differences between the binding sites of protein and PI3 kinases, both are able to bind an overlapping range of fragments. As the compound set was designed primarily to target protein kinases, it is not possible to say from our results whether lipid kinases can routinely bind chemotypes other than those expected to target protein kinases.

To conclude, both PIM1 and the PI3 kinases are highly tractable targets for FBDD. Fragments designed to bind to the hinge region of typical protein kinases are rich in potential starting points for these targets.

## DISCUSSION

The main aim behind the creation of this fragment set was to discover hits for lead optimization. In this, the approach was highly successful, with multiple hits found against all kinases screened. These include targets very different from those envisaged when the set was created, and the FBDD approach seems well suited to atypical kinases such as PIM1 and the PI3 kinases.



Numerous hinge-binding fragments of typical protein kinases also bind to these targets, although because of differences elsewhere in their ATP-binding sites, we expect that optimization to selective molecules should be possible.

Here we have highlighted general points of interest learned from the exercise. First, we gained insights into strategies for fragment screening and detection. We believe that to gain confidence to embark on the optimization of a fragment hit, it is important to demonstrate both target engagement and inhibition of kinase activity. Binding is necessary but may not be sufficient if, for example, the compound binds to a site with no functional relevance. Biochemical screens are typically high throughput and in an industrial setting are generally already in existence for other hit-finding approaches when a fragment screen is run. Even if these may need to be reconfigured and checked for suitability as a high-compound concentration screen, the resource required to screen a fragment set through them is likely to be relatively low.

Therefore, we used a biochemical screen as the first pass in our fragment cascade, followed by IC<sub>50</sub> confirmation. This may have disadvantages if the biochemical assay is prone to interference, but the impact of this can be reduced. We have shown that the degree of interference varies between different screening techniques, and some are quite insensitive to artifacts. Even the assays with the highest interference rates gave useful hits that could be triaged readily by a lower-throughput approach. As many of these artifacts arise from compound fluorescence, biochemical assays that do not rely on fluorescent readouts (e.g., MS) may provide an even better solution. Having obtained the biochemical readout, lower-throughput biophysical methods were used to confirm on-target binding of as many of the hits as possible (e.g., an NMR STD experiment in our PDK1 example<sup>25</sup>).

Second, we gained experience in prioritizing fragment hits for progression. It is intuitively attractive to begin to optimize the most ligand-efficient starting points. However, our set typically yielded many hits with comparable efficiency, and it is difficult to say in advance which will retain this during optimization. Potent literature inhibitors frequently contain hinge-binding fragments that themselves show only relatively low efficiency for their target. We therefore found it beneficial to carry as many fragments as possible through to the biophysical confirmation step.

Confirmed binders then formed the basis for substructure searches in databases of available molecules. Analogues from these searches were useful in many ways, from learning about the SAR of the template to allowing the determination of X-ray structures when attempts to crystallize the initial fragment failed. With the SAR information in hand, the chemical tractability of each template was assessed. To assist in this, information about the fragments' binding mode was used in order to consider the opportunities for making them more potent and selective. When crystallography is not available, kinases represent a special class where it is sometimes possible to infer the binding mode with some confidence using information from related fragments in other kinases.<sup>14,83</sup>

Third, we gained insights into the selectivity profiles of kinase hinge-binding fragments. They show complex profiles analogous to those of larger inhibitors, so it is not surprising that making use of this information is complex and difficult to generalize. It is appealing to prioritize more selective starting points over unselective ones. However, one of our findings is that selective inhibitors can be made from unselective hinge-binding starting points and that compounds containing selective hinge-binding fragments are not necessarily selective themselves. From this, it

follows that a given fragment can be used as a starting point for making inhibitors of multiple kinases. Therefore, one valuable outcome of fragment profiling is the identification of novel hinge-binding templates that can form the basis for pan-kinase system-based arrays of leadlike molecules. It is likely that these will have properties (selectivity, DMPK, etc.) that are more predictive of the properties of optimized compounds than the fragments.

We have also learned about the selectivity profiles of fragments that bind outside the ATP-binding site, especially those targeting the DFG-out conformation. These inhibited p38 $\alpha$  and B-Raf but not other kinases from our panel. Even if this is due to our choice of fragments, assay format or the protein activation state, rather than intrinsic differences between the kinases, it seems that developing potent and efficient inhibitors that bind in this manner to the other kinases in our panel might be challenging.

Finally, we note that pairs of fragments with high field similarity are likely to share similar kinase profiles. This suggests that this approach might be a useful way to identify novel alternatives with similar profiles to known fragments.

As with other approaches, fragment-based drug discovery has been established for some time as a successful strategy for kinases. The wealth of information available about the binding determinants for the kinase ATP site makes a focused approach particularly attractive for this target class. We and others have demonstrated the broad utility of the strategy to discover starting points for multiple kinases. Here we have focused on learnings gained from the exercise, and the application of this approach to specific targets of interest will be the subject of future publications.

## METHODS

**Targeted Fragment Set Creation.** The initial purpose for the creation and screening of this set was to find backup leads for IKK $\beta$ . Focused screening had identified fragment hits that had been successfully optimized without the aid of a crystal structure,<sup>83</sup> so it was decided to extend the approach by assembling a set of fragment-sized molecules targeting mainly but not exclusively the ATP site. This was also made available for screening against other kinases.

The set was constructed using public and proprietary knowledge about the kinase system. Briefly, the selection of compounds was carried out as follows:

- (1) A list of plentifully available solid samples was assembled from the GSK collection and from external suppliers. An initial cutoff of 25 or fewer heavy atoms was used to reduce the list to a manageable number. Although step 5 below resulted in most fragments chosen being much smaller than this, some exceptions were included through step 6.
- (2) A list of >300 filters for reactive or undesirable functional groups was applied. These substructures were based on the evolving experience of GSK medicinal chemists over time and include, for example, electrophilic groups liable to interact irreversibly with biomolecules or features that are unstable to storage, which would complicate interpretation of the results.<sup>84</sup>
- (3) Crude substructure filters were applied to discard structures without any suitable kinase hinge-binding hydrogen-bond acceptor functional group. These groups include aromatic nitrogen atoms, other sp<sup>2</sup> ring nitrogen atoms that are not formally aromatic, phenolic oxygen or sp<sup>2</sup> oxygen atoms adjacent to a ring, and cyclic and acyclic amides. The overwhelming majority of crystal structures of potent ATP-site inhibitors of typical kinases show a hydrogen-bonding interaction between one of these groups and the hinge residue backbone.

- (4) A 3D-pharmacophore approach was then used to flag which of the remaining 18 000 candidate fragments contain a hinge-binding H-bond acceptor group backed by a hydrophobic ring. No H-bond donor feature was enforced. Excluded volume spheres were added to describe the approximate shape of a generic ATP site. This pharmacophore was used to mark fragments to help to prioritize their selection in step 5 but was not used as an absolute filter.
- (5) The fragments were clustered by a variety of cheminformatic methods and examined one cluster at a time, taking account of the pharmacophore information and the precedent of similar fragments occurring as hinge-binding groups in kinase crystal structures. A subjective selection was made taking account of "rule of three" principles as guidelines.<sup>85</sup>
- (6) A small number of additional fragments not targeted at the ATP site were added. These include fragments directed at known allosteric pockets as well as other simple groups lacking the hinge-binding hydrogen bond. Some of these compounds fall outside the space recommended by the rule of three guidelines but were included regardless, as they could provide useful information.

**Set Creation and QC.** A total of 1065 compounds were selected and dissolved in DMSO to 10 mM before being subjected to LC–MS quality analysis. Compounds not matching the reported structure were submitted for NMR structural analysis. Compounds with less than 90% purity by LC–MS were still screened, and indeed some provided hits that were later validated crystallographically. The data reported here were gathered over a period of over a year, after which the QC analysis was repeated. Data from compounds failing QC have been excluded from this analysis, which only considers the 936 compounds that retained their structural integrity throughout the entire process.

Properties of the set (MW, cLogP, H-bond acceptor and donor counts) are shown in Supporting Information, Figure S6.

**Assays.** Thirty assays using a variety of formats were used: FP (fluorescence polarization, measuring the displacement of fluorescently tagged ATP-competitive inhibitors) and activity-based, measuring the inhibition of phosphorylation, using TR-FRET, IMAP, and LEADseeker formats. More detailed descriptions of the 30 assays can be found in Supporting Information Figure S3. Briefly, in all activity-based screens the ATP concentration was at or below the  $K_m$  for the kinase. Compounds were dissolved in buffer to a final concentration of either 400 or 667  $\mu\text{M}$ , and the percentage inhibition or binding was measured. Percent inhibition values have been used rather than measures of ligand efficiency,<sup>47</sup> as the aim is to compare compounds across different assays. Full data are given in Supporting Information. For all but one kinase, the results are expressed as the mean of at least two runs.

The assays were carried out under different conditions, so neither % I nor ligand efficiency scores is strictly comparable. The activity based assays were carried out with [ATP] at or below the  $K_m$  of the kinase, so they should be roughly equivalent (assuming ATP competition, they show a <2-fold shift of  $\text{IC}_{50}$  relative to  $K_i$  following the Cheng–Prusoff relationship). Binding (fluorescence polarization, FP) assays are generally run with a slightly larger (3- to 5-fold) shift in  $\text{IC}_{50}$  relative to  $K_i$ . Thus, a theoretical ATP-competitive inhibitor screened at a concentration equal to its  $K_i$  against all the kinases in the panel would show inhibition in the range 20–50% (33% for those with [ATP] =  $K_m$ ). In this situation, % I values will be very sensitive to small changes in compound concentration, so small differences will not be significant. As it is impossible to estimate an  $\text{IC}_{50}$  when a compound's % I values are close to zero or 100%, nothing can be said about the relative activity of two such compounds.  $\text{IC}_{50}$  values would give a more precise measure of affinity, but as these are more time-consuming to measure, many groups carry out kinase cross-profiling at a single concentration before following up results of interest at full curve. However, because the % I seems to be

fairly predictive of  $\text{IC}_{50}$  (e.g., Supporting Information, Figure S1c), the precision of these results should be sufficient to support our conclusions.

#### Comparison of Fragments and Lead-Sized Molecules.

Fragments were first cleaned by removing groups judged to be unfunctional. This process removes all halogen atoms and pendent acyclic alkyl or ether chains. In general there were few such groups in the set, as fragments containing them were only included if no analogues without them were available. Removal of such groups was needed because where they do appear in fragments they frequently occur in positions that are substituted in the elaborated molecules. The resulting cleaned fragments were used as individual SMARTS input to carry out substructure searches against the data set of lead-sized molecules using the Daylight toolkit.<sup>86</sup> Hits were then associated with the fragments from which they were derived. Visual inspection of the hits and the substructures was carried out to confirm that the fragment was present in the associated compounds and not masked by inappropriate substitution (so that the hinge-binding hydrogen bonds were still accessible, for example).

**Activity Similarity.** The activity similarity score between pairs of fragments was calculated as follows, in a similar way as in our previous publication describing lead-sized molecules.<sup>20</sup> The profile of each compound is reduced to a bit string where each bit represents activity (1) or inactivity (0). Activity is decided using a fixed activity threshold: results shown are from a cutoff of 30% inhibition, but other values gave the same conclusions. The activity similarity between a pair of fragments is the Tanimoto coefficient of the two profile bit strings and ranges between 0 (dissimilar) to 1 (similar).

**Field Similarity.** Field similarity scores between pairs of fragments were calculated as follows. Fragments were built in 3D, with enumeration of tautomers and undefined chiral centers, using LIGPREP.<sup>87</sup> Each structure was compared to every other, using the Fastqmf module of FieldScreen.<sup>88</sup> The greatest score for all combinations of conformers or tautomers was taken as the similarity score between fragments.

## ■ ASSOCIATED CONTENT

**S Supporting Information.** A pdf file containing Figures S1–S6 showing validation, correlation coefficients, assay types and hit rates, box-plot version of Figure 6, similarity scores, and property distribution; a text file containing % inhibition results for 936 compounds profiled against 30 kinases. This material is available free of charge via the Internet at <http://pubs.acs.org>.

## ■ AUTHOR INFORMATION

### Corresponding Author

\*Phone: +44 1348 745745. Fax: +44 1438 764502. E-mail: Paul.A.Bamborough@gsk.com.

### Present Addresses

<sup>†</sup>Heptares Therapeutics Limited, BioPark, Welwyn Garden City, Hertfordshire, AL7 3AX, UK.

## ■ ACKNOWLEDGMENT

We thank Brian Hardy for compound handling and set creation, Neha Mittal for QC analysis, Andy Roberts for NMR analysis, and all the members of the Screening and Compound Profiling group who performed the assays.

## ■ ABBREVIATIONS USED

FBDD, fragment-based drug discovery; FP, fluorescence polarization; IMAP, immobilized metal affinity phosphorylation; LE,

ligand efficiency; SPR, surface plasmon resonance; TR-FRET, time-resolved fluorescence resonance energy transfer

## REFERENCES

- (1) Hann, M. M.; Leach, A. R.; Harper, G. Molecular complexity and its impact on the probability of finding leads for drug discovery. *J. Chem. Inf. Comput. Sci.* **2001**, *41*, 856–864.
- (2) Congreve, M.; Chessari, G.; Tisi, D.; Woodhead, A. J. Recent developments in fragment-based drug discovery. *J. Med. Chem.* **2008**, *51*, 3661–3680.
- (3) de Kloe, G. E.; Bailey, D.; Leurs, R.; de Esch, I. J. Transforming fragments into candidates: small becomes big in medicinal chemistry. *Drug Discovery Today* **2009**, *14*, 630–646.
- (4) Erlanson, D. A.; McDowell, R. S.; O'Brien, T. Fragment-based drug discovery. *J. Med. Chem.* **2004**, *47*, 3463–3482.
- (5) Fejzo, J.; Lepre, C. A.; Peng, J. W.; Bemis, G. W.; Ajay, Murcko, M. A.; Moore, J. M. The SHAPES strategy: an NMR-based approach for lead generation in drug discovery. *Chem. Biol.* **1999**, *6*, 755–769.
- (6) Fejzo, J.; Lepre, C.; Xie, X. Application of NMR screening in drug discovery. *Curr. Top. Med. Chem.* **2003**, *3*, 81–97.
- (7) Hartshorn, M. J.; Murray, C. W.; Cleasby, A.; Frederickson, M.; Tickle, I. J.; Jhoti, H. Fragment-based lead discovery using X-ray crystallography. *J. Med. Chem.* **2005**, *48*, 403–413.
- (8) Gill, A. L.; Frederickson, M.; Cleasby, A.; Woodhead, S. J.; Carr, M. G.; Woodhead, A. J.; Walker, M. T.; Congreve, M. S.; Devine, L. A.; Tisi, D.; O'Reilly, M.; Seavers, L. C.; Davis, D. J.; Curry, J.; Anthony, R.; Padova, A.; Murray, C. W.; Carr, R. A.; Jhoti, H. Identification of novel p38alpha MAP kinase inhibitors using fragment-based lead generation. *J. Med. Chem.* **2005**, *48*, 414–426.
- (9) Baurin, N.; Aboul-Ela, F.; Barril, X.; Davis, B.; Drysdale, M.; Dymock, B.; Finch, H.; Fromont, C.; Richardson, C.; Simmonite, H.; Hubbard, R. E. Design and characterization of libraries of molecular fragments for use in NMR screening against protein targets. *J. Chem. Inf. Comput. Sci.* **2004**, *44*, 2157–2166.
- (10) Warner, S. L.; Bashyam, S.; Vankayalapati, H.; Bearss, D. J.; Han, H.; Mahadevan, D.; Von Hoff, D. D.; Hurley, L. H. Identification of a lead small-molecule inhibitor of the Aurora kinases using a structure-assisted, fragment-based approach. *Mol. Cancer Ther.* **2006**, *5*, 1764–1773.
- (11) Howard, S.; Berdini, V.; Boulstridge, J. A.; Carr, M. G.; Cross, D. M.; Curry, J.; Devine, L. A.; Early, T. R.; Fazal, L.; Gill, A. L.; Heathcote, M.; Maman, S.; Matthews, J. E.; McMenamin, R. L.; Navarro, E. F.; O'Brien, M. A.; O'Reilly, M.; Rees, D. C.; Reule, M.; Tisi, D.; Williams, G.; Vinkovic, M.; Wyatt, P. G. Fragment-based discovery of the pyrazol-4-yl urea (AT9283), a multitargeted kinase inhibitor with potent aurora kinase activity. *J. Med. Chem.* **2009**, *52*, 379–388.
- (12) Keminer, O.; Kraemer, J.; Kahmann, J.; Sternberger, I.; Scheich, C.; Jungmann, J.; Schaert, S.; Winkler, D.; Ichihara, O.; Whittaker, M.; Ullmann, D.; Hestekamp, T. Novel MK2 inhibitors by fragment screening. *Comb. Chem. High Throughput Screening* **2009**, *12*, 697–703.
- (13) Matthews, T. P.; Klair, S.; Burns, S.; Boxall, K.; Cherry, M.; Fisher, M.; Westwood, I. M.; Walton, M. I.; McHardy, T.; Cheung, K. M.; van Montfort, R.; Williams, D.; Aherne, G. W.; Garrett, M. D.; Reader, J.; Collins, I. Identification of inhibitors of checkpoint kinase 1 through template screening. *J. Med. Chem.* **2009**, *52*, 4810–4819.
- (14) Ray, P.; Wright, J.; Adam, J.; Boucharens, S.; Black, D.; Brown, A. R.; Epemolu, O.; Fletcher, D.; Huggett, M.; Jones, P.; Laats, S.; Lyons, A.; Man, J.; Morphy, R.; Sherborne, B.; Sherry, L.; Straten, N.; Westwood, P.; York, M. Optimisation of 6-substituted isoquinolin-1-amine based ROCK-I inhibitors. *Bioorg. Med. Chem. Lett.* **2011**, *21*, 1084–1088.
- (15) Lesuisse, D.; Mauger, J.; Nemecek, C.; Maignan, S.; Boiziau, J.; Harlow, G.; Hittinger, A.; Ruf, S.; Strobel, H.; Nair, A.; Ritter, K.; Malleron, J.-L.; Degallier, A.; El-Ahmad, Y.; Guilloteau, J.-P.; Guizani, H.; Bouchard, H.; Venot, C. Discovery of the first non-ATP competitive IGF-1R inhibitors: advantages in comparison with competitive inhibitors. *Bioorg. Med. Chem. Lett.* **2011**, *21*, 2224–2228.
- (16) Barelier, S.; Pons, J.; Gehring, K.; Lancelin, J. M.; Krimm, I. Ligand specificity in fragment-based drug design. *J. Med. Chem.* **2010**, *53*, 5256–5266.
- (17) Chen, Y.; Shoichet, B. K. Molecular docking and ligand specificity in fragment-based inhibitor discovery. *Nat. Chem. Biol.* **2009**, *5*, 358–364.
- (18) Fabian, M. A.; Biggs, W. H., III; Treiber, D. K.; Atteridge, C. E.; Azimioara, M. D.; Benedetti, M. G.; Carter, T. A.; Ciceri, P.; Edeen, P. T.; Floyd, M.; Ford, J. M.; Galvin, M.; Gerlach, J. L.; Grotzfeld, R. M.; Herrgard, S.; Insko, D. E.; Insko, M. A.; Lai, A. G.; Lelias, J. M.; Mehta, S. A.; Milanov, Z. V.; Velasco, A. M.; Wodicka, L. M.; Patel, H. K.; Zarrinkar, P. P.; Lockhart, D. J. A small molecule-kinase interaction map for clinical kinase inhibitors. *Nat. Biotechnol.* **2005**, *23*, 329–336.
- (19) Fedorov, O.; Marsden, B.; Pogacic, V.; Rellos, P.; Muller, S.; Bullock, A. N.; Schwaller, J.; Sundstrom, M.; Knapp, S. A systematic interaction map of validated kinase inhibitors with Ser/Thr kinases. *Proc. Natl. Acad. Sci. U.S.A.* **2007**, *104*, 20523–20528.
- (20) Bamborough, P.; Drewry, D.; Harper, G.; Smith, G. K.; Schneider, K. Assessment of chemical coverage of kinome space and its implications for kinase drug discovery. *J. Med. Chem.* **2008**, *51*, 7898–7914.
- (21) Smyth, L. A.; Collins, I. Measuring and interpreting the selectivity of protein kinase inhibitors. *J. Chem. Biol.* **2009**, *2*, 131–151.
- (22) Schuffenhauer, A.; Ruedisser, S.; Marzinzik, A. L.; Jahnke, W.; Blommers, M.; Selzer, P.; Jacoby, E. Library design for fragment based screening. *Curr. Top. Med. Chem.* **2005**, *5*, 751–762.
- (23) Jacoby, E.; Davies, J.; Blommers, M. J. Design of small molecule libraries for NMR screening and other applications in drug discovery. *Curr. Top. Med. Chem.* **2003**, *3*, 11–23.
- (24) Siegal, G.; Ab, E.; Schultz, J. Integration of fragment screening and library design. *Drug Discovery Today* **2007**, *12*, 1032–1039.
- (25) Medina, J. R.; Blackledge, C. W.; Heering, D. A.; Campobasso, N.; Ward, P.; Briand, J.; Wright, L.; Axten, J. M. Aminoindazole PDK1 inhibitors: a case study in fragment-based drug discovery. *ACS Med. Chem. Lett.* **2010**, *20*, 2552–2555.
- (26) Shapiro, A. B.; Walkup, G. K.; Keating, T. A. Correction for interference by test samples in high-throughput assays. *J. Biomol. Screening* **2009**, *14*, 1008–1016.
- (27) Jadhav, A.; Ferreira, R. S.; Klumpp, C.; Mott, B. T.; Austin, C. P.; Inglese, J.; Thomas, C. J.; Maloney, D. J.; Shoichet, B. K.; Simeonov, A. Quantitative analyses of aggregation, autofluorescence, and reactivity artifacts in a screen for inhibitors of a thiol protease. *J. Med. Chem.* **2010**, *53*, 37–51.
- (28) Boehm, H. J.; Boehringer, M.; Bur, D.; Gmuender, H.; Huber, W.; Klaus, W.; Kostrewa, D.; Kuehne, H.; Luebbbers, T.; Meunier-Keller, N.; Mueller, F. Novel inhibitors of DNA gyrase: 3D structure based biased needle screening, hit validation by biophysical methods, and 3D guided optimization. A promising alternative to random screening. *J. Med. Chem.* **2000**, *43*, 2664–2674.
- (29) Shuker, S. B.; Hajduk, P. J.; Meadows, R. P.; Fesik, S. W. Discovering high-affinity ligands for proteins: SAR by NMR. *Science* **1996**, *274*, 1531–1534.
- (30) Siegal, G.; Hollander, J. G. Target immobilization and NMR screening of fragments in early drug discovery. *Curr. Top. Med. Chem.* **2009**, *9*, 1736–1745.
- (31) Dalvit, C. NMR methods in fragment screening: theory and a comparison with other biophysical techniques. *Drug Discovery Today* **2009**, *14*, 1051–1057.
- (32) Nienaber, V. L.; Richardson, P. L.; Klighofer, V.; Bouska, J. J.; Giranda, V. L.; Greer, J. Discovering novel ligands for macromolecules using X-ray crystallographic screening. *Nat. Biotechnol.* **2000**, *18*, 1105–1108.
- (33) Perspicace, S.; Banner, D.; Benz, J.; Muller, F.; Schlatter, D.; Huber, W. Fragment-based screening using surface plasmon resonance technology. *J. Biomol. Screening* **2009**, *14*, 337–349.
- (34) Hamalainen, M. D.; Zhukov, A.; Ivarsson, M.; Fex, T.; Gottfries, J.; Karlsson, R.; Bjorsne, M. Label-free primary screening and affinity ranking of fragment libraries using parallel analysis of protein panels. *J. Biomol. Screening* **2008**, *13*, 202–209.
- (35) Elinder, M.; Geitmann, M.; Gossas, T.; Kallblad, P.; Winqvist, J.; Nordstrom, H.; Hamalainen, M.; Danielson, U. H. Experimental

validation of a fragment library for lead discovery using SPR biosensor technology. *J. Biomol. Screening* **2011**, *16*, 15–25.

(36) Kobayashi, M.; Retra, K.; Figaroa, F.; Hollander, J. G.; Ab, E.; Heetebrij, R. J.; Irth, H.; Siegal, G. Target immobilization as a strategy for NMR-based fragment screening: comparison of TINS, STD, and SPR for fragment hit identification. *J. Biomol. Screening* **2010**, *15*, 978–989.

(37) Boettcher, A.; Ruedisser, S.; Erbel, P.; Vinzenz, D.; Schiering, N.; Hassiepen, U.; Rigollier, P.; Mayr, L. M.; Woelcke, J. Fragment-based screening by biochemical assays: systematic feasibility studies with trypsin and MMP12. *J. Biomol. Screening* **2010**, *15*, 1029–1041.

(38) Vieth, M.; Higgs, R. E.; Robertson, D. H.; Shapiro, M.; Gragg, E. A.; Hemmerle, H. Kinomics-structural biology and chemogenomics of kinase inhibitors and targets. *Biochim. Biophys. Acta* **2004**, *1697*, 243–257.

(39) Posy, S. L.; Hermsmeier, M. A.; Vaccaro, W.; Ott, K. H.; Todderud, G.; Lippy, J. S.; Trainor, G. L.; Loughney, D. A.; Johnson, S. R. Trends in kinase selectivity: insights for target class-focused library screening. *J. Med. Chem.* **2011**, *54*, 54–66.

(40) Gaudet, E. A.; Huang, K. S.; Zhang, Y.; Huang, W.; Mark, D.; Sportsman, J. R. A homogeneous fluorescence polarization assay adaptable for a range of protein serine/threonine and tyrosine kinases. *J. Biomol. Screening* **2003**, *8*, 164–175.

(41) Beveridge, M.; Park, Y. W.; Hermes, J.; Marengi, A.; Brophy, G.; Santos, A. Detection of p56(lck) kinase activity using scintillation proximity assay in 384-well format and imaging proximity assay in 384- and 1536-well format. *J. Biomol. Screening* **2000**, *5*, 205–212.

(42) Aliagas-Martin, I.; Burdick, D.; Corson, L.; Dotson, J.; Drummond, J.; Fields, C.; Huang, O. W.; Hunsaker, T.; Kleinheinz, T.; Krueger, E.; Liang, J.; Moffat, J.; Phillips, G.; Pulk, R.; Rawson, T. E.; Ultsch, M.; Walker, L.; Wiesmann, C.; Zhang, B.; Zhu, B. Y.; Cochran, A. G. A class of 2,4-bisanilinopyrimidine Aurora A inhibitors with unusually high selectivity against Aurora B. *J. Med. Chem.* **2009**, *52*, 3300–3307.

(43) Tavares, F. X.; Boucheron, J. A.; Dickerson, S. H.; Griffin, R. J.; Preugschat, F.; Thomson, S. A.; Wang, T. Y.; Zhou, H. Q. N-Phenyl-4-pyrazolo[1,5-*b*]pyridazin-3-ylpyrimidin-2-amines as potent and selective inhibitors of glycogen synthase kinase 3 with good cellular efficacy. *J. Med. Chem.* **2004**, *47*, 4716–4730.

(44) Liu, M.; Wang, S.; Clampit, J. E.; Gum, R. J.; Haasch, D. L.; Rondinone, C. M.; Trevillyan, J. M.; Abad-Zapatero, C.; Fry, E. H.; Sham, H. L.; Liu, G. Discovery of a new class of 4-anilinopyrimidines as potent c-Jun N-terminal kinase inhibitors: synthesis and SAR studies. *Bioorg. Med. Chem. Lett.* **2007**, *17*, 668–672.

(45) Adams, J. L.; Boehm, J. C.; Gallagher, T. F.; Kassis, S.; Webb, E. F.; Hall, R.; Sorenson, M.; Garigipati, R.; Griswold, D. E.; Lee, J. C. Pyrimidinylimidazole inhibitors of p38: cyclic N-1 imidazole substituents enhance p38 kinase inhibition and oral activity. *Bioorg. Med. Chem. Lett.* **2001**, *11*, 2867–2870.

(46) Bingham, A. H.; Davenport, R. J.; Gowers, L.; Knight, R. L.; Lowe, C.; Owen, D. A.; Parry, D. M.; Pitt, W. R. A novel series of potent and selective IKK2 inhibitors. *Bioorg. Med. Chem. Lett.* **2004**, *14*, 409–412.

(47) Abad-Zapatero, C. Ligand efficiency indices for effective drug discovery. *Expert Opin. Drug Discovery* **2007**, *2* (4), 469–488.

(48) Donald, A.; McHardy, T.; Rowlands, M. G.; Hunter, L. J.; Davies, T. G.; Berdini, V.; Boyle, R. G.; Aherne, G. W.; Garrett, M. D.; Collins, I. Rapid evolution of 6-phenylpurine inhibitors of protein kinase B through structure-based design. *J. Med. Chem.* **2007**, *50*, 2289–2292.

(49) Guengerich, F. P.; Sorrells, J. L.; Schmitt, S.; Krauser, J. A.; Aryal, P.; Meijer, L. Generation of new protein kinase inhibitors utilizing cytochrome p450 mutant enzymes for indigoid synthesis. *J. Med. Chem.* **2004**, *47*, 3236–3241.

(50) Davies, T. G.; Woodhead, S. J.; Collins, I. Fragment-based discovery of inhibitors of protein kinase B. *Curr. Top. Med. Chem.* **2009**, *9*, 1705–1717.

(51) Seefeld, M. A.; Rouse, M. B.; McNulty, K. C.; Sun, L.; Wang, J.; Yamashita, D. S.; Luengo, J. I.; Zhang, S.; Minthorn, E. A.; Concha, N. O.; Heerding, D. A. Discovery of 5-pyrrolopyridinyl-2-thiophene-carboxamides as potent AKT kinase inhibitors. *Bioorg. Med. Chem. Lett.* **2009**, *19*, 2244–2248.

(52) Hammond, M.; Washburn, D. G.; Hoang, H. T.; Manns, S.; Frazee, J. S.; Nakamura, H.; Patterson, J. R.; Trizna, W.; Wu, C.; Azzarano, L. M.; Nagilla, R.; Nord, M.; Trejo, R.; Head, M. S.; Zhao, B.; Smallwood, A. M.; Hightower, K.; Laping, N. J.; Schnackenberg, C. G.; Thompson, S. K. Design and synthesis of orally bioavailable serum and glucocorticoid-regulated kinase 1 (SGK1) inhibitors. *Bioorg. Med. Chem. Lett.* **2009**, *19*, 4441–4445.

(53) Liddle, J.; Bamborough, P.; Barker, M. D.; Campos, S.; Cousins, R. P.; Cutler, G. J.; Hobbs, H.; Holmes, D. S.; Ioannou, C.; Mellor, G. W.; Morse, M. A.; Payne, J. J.; Pritchard, J. M.; Smith, K. J.; Tape, D. T.; Whitworth, C.; Williamson, R. A. 4-Phenyl-7-azaindoles as potent and selective IKK2 inhibitors. *Bioorg. Med. Chem. Lett.* **2009**, *19*, 2504–2508.

(54) Graczyk, P.; Khan, A.; Bhatia, G.; Imura, Y. Preparation of Pyrrolo[2,3-*b*]pyrimidines as Inhibitors of c-Jun N-Terminal Kinases (JNKs) Inhibitors for the Treatment of Neurodegenerative Disorders. WO 2004078756, 2004.

(55) Wyatt, P. G.; Woodhead, A. J.; Berdini, V.; Boulstridge, J. A.; Carr, M. G.; Cross, D. M.; Davis, D. J.; Devine, L. A.; Early, T. R.; Feltell, R. E.; Lewis, E. J.; McMenamin, R. L.; Navarro, E. F.; O'Brien, M. A.; O'Reilly, M.; Reule, M.; Saxty, G.; Seavers, L. C.; Smith, D. M.; Squires, M. S.; Trewartha, G.; Walker, M. T.; Woolford, A. J. Identification of N-(4-piperidinyl)-4-(2,6-dichlorobenzoylamino)-1H-pyrazole-3-carboxamide (AT7519), a novel cyclin dependent kinase inhibitor using fragment-based X-ray crystallography and structure based drug design. *J. Med. Chem.* **2008**, *51*, 4986–4999.

(56) Zhu, G. D.; Gandhi, V. B.; Gong, J.; Thomas, S.; Woods, K. W.; Song, X.; Li, T.; Diebold, R. B.; Luo, Y.; Liu, X.; Guan, R.; Klinghofer, V.; Johnson, E. F.; Bouska, J.; Olson, A.; Marsh, K. C.; Stoll, V. S.; Mamo, M.; Polakowski, J.; Campbell, T. J.; Martin, R. L.; Gintant, G. A.; Penning, T. D.; Li, Q.; Rosenberg, S. H.; Giranda, V. L. Syntheses of potent, selective, and orally bioavailable indazole-pyridine series of protein kinase B/Akt inhibitors with reduced hypotension. *J. Med. Chem.* **2007**, *50*, 2990–3003.

(57) Hajduk, P. J. Fragment-based drug design: How big is too big? *J. Med. Chem.* **2006**, *49*, 6972–6976.

(58) Babaoglu, K.; Shoichet, B. K. Deconstructing fragment-based inhibitor discovery. *Nat. Chem. Biol.* **2006**, *2*, 720–723.

(59) Karaman, M. W.; Herrgard, S.; Treiber, D. K.; Gallant, P.; Atteridge, C. E.; Campbell, B. T.; Chan, K. W.; Ciceri, P.; Davis, M. I.; Edeen, P. T.; Faraoni, R.; Floyd, M.; Hunt, J. P.; Lockhart, D. J.; Milanov, Z. V.; Morrison, M. J.; Pallares, G.; Patel, H. K.; Pritchard, S.; Wodicka, L. M.; Zarrinkar, P. P. A quantitative analysis of kinase inhibitor selectivity. *Nat. Biotechnol.* **2008**, *26*, 127–132.

(60) Cheeseright, T. J.; Holm, M.; Lehmann, F.; Luik, S.; Gottert, M.; Melville, J. L.; Laufer, S. Novel lead structures for p38 MAP kinase via FieldScreen virtual screening. *J. Med. Chem.* **2009**, *52*, 4200–4209.

(61) Antonyamy, S.; Hirst, G.; Park, F.; Sprengeler, P.; Stappenbeck, F.; Steensma, R.; Wilson, M.; Wong, M. Fragment-based discovery of JAK-2 inhibitors. *Bioorg. Med. Chem. Lett.* **2009**, *19*, 279–282.

(62) Filippakopoulos, P.; Rellos, P.; Fedorov, O.; Niesen, F.; Pike, A. C. W.; Pilka, E.; von Delft, F.; Arrowsmith, C. H.; Edwards, A.; Weigelt, J.; Knapp, S. Unpublished results, PDB entry 3BQR, 2010.

(63) Fitzgerald, C. E.; Patel, S. B.; Becker, J. W.; Cameron, P. M.; Zaller, D.; Pikounis, V. B.; O'Keefe, S. J.; Scapin, G. Structural basis for p38 $\alpha$  MAP kinase quinazolinone and pyridol-pyrimidine inhibitor specificity. *Nat. Struct. Biol.* **2003**, *10*, 764–769.

(64) Pogacic, V.; Bullock, A. N.; Fedorov, O.; Filippakopoulos, P.; Gasser, C.; Biondi, A.; Meyer-Monard, S.; Knapp, S.; Schwaller, J. Structural analysis identifies imidazo[1,2-*b*]pyridazines as PIM kinase inhibitors with in vitro antileukemic activity. *Cancer Res.* **2007**, *67*, 6916–6924.

(65) Saxty, G.; Woodhead, S. J.; Berdini, V.; Davies, T. G.; Verdonk, M. L.; Wyatt, P. G.; Boyle, R. G.; Barford, D.; Downham, R.; Garrett, M. D.; Carr, R. A. Identification of inhibitors of protein kinase B using fragment-based lead discovery. *J. Med. Chem.* **2007**, *50*, 2293–2296.

(66) Pargellis, C.; Tong, L.; Churchill, L.; Cirillo, P. F.; Gilmore, T.; Graham, A. G.; Grob, P. M.; Hickey, E. R.; Moss, N.; Pav, S.; Regan, J. Inhibition of p38 MAP kinase by utilizing a novel allosteric binding site. *Nat. Struct. Biol.* **2002**, *9*, 268–272.

- (67) Schindler, T.; Bornmann, W.; Pellicena, P.; Miller, W. T.; Clarkson, B.; Kuriyan, J. Structural mechanism for STI-571 inhibition of abelson tyrosine kinase. *Science* **2000**, *289*, 1938–1942.
- (68) Smith, R. A.; Barbosa, J.; Blum, C. L.; Bobko, M. A.; Caringal, Y. V.; Dally, R.; Johnson, J. S.; Katz, M. E.; Kennure, N.; Kingery-Wood, J.; Lee, W.; Lowinger, T. B.; Lyons, J.; Marsh, V.; Rogers, D. H.; Swartz, S.; Walling, T.; Wild, H. Discovery of heterocyclic ureas as a new class of raf kinase inhibitors: identification of a second generation lead by a combinatorial chemistry approach. *Bioorg. Med. Chem. Lett.* **2001**, *11*, 2775–2778.
- (69) Regan, J.; Capolino, A.; Cirillo, P. F.; Gilmore, T.; Graham, A. G.; Hickey, E.; Kroe, R. R.; Madwed, J.; Moriak, M.; Nelson, R.; Pargellis, C. A.; Swinamer, A.; Torcellini, C.; Tang, M.; Moss, N. Structure–activity relationships of the p38 $\alpha$  MAP kinase inhibitor 1-(5-*tert*-butyl-2-*p*-tolyl-2*H*-pyrazol-3-yl)-3-[4-(2-morpholin-4-yl-ethoxy)naphthalen-1-yl]urea (BIRB 796). *J. Med. Chem.* **2003**, *46*, 4676–4686.
- (70) Angell, R. M.; Angell, T. D.; Bamborough, P.; Bamford, M. J.; Chung, C. W.; Cockerill, S. G.; Flack, S. S.; Jones, K. L.; Laine, D. I.; Longstaff, T.; Ludbrook, S.; Pearson, R.; Smith, K. J.; Smees, P. A.; Somers, D. O.; Walker, A. L. Biphenyl amide p38 kinase inhibitors 4: DFG-in and DFG-out binding modes. *Bioorg. Med. Chem. Lett.* **2008**, *18*, 4433–4437.
- (71) Erlanson, D. A.; Arndt, J. W.; Cancilla, M. T.; Cao, K.; Elling, R. A.; English, N.; Friedman, J.; Hansen, S. K.; Hession, C.; Joseph, I.; Kumaravel, G.; Lee, W. C.; Lind, K. E.; McDowell, R. S.; Miatkowski, K.; Nguyen, C.; Nguyen, T. B.; Park, S.; Pathan, N.; Penny, D. M.; Romanowski, M. J.; Scott, D.; Silvian, L.; Simmons, R. L.; Tangonan, B. T.; Yang, W.; Sun, L. Discovery of a potent and highly selective PDK1 inhibitor via fragment-based drug discovery. *Bioorg. Med. Chem. Lett.* **2011**, *21*, 3078–3083.
- (72) Nagashima, K.; Shumway, S. D.; Sathyanarayanan, S.; Chen, A. H.; Dolinski, B.; Xu, Y.; Keilhack, H.; Nguyen, T.; Wiznerowicz, M.; Li, L.; Lutterbach, B. A.; Chi, A.; Paweletz, C.; Allison, T.; Yan, Y.; Munshi, S. K.; Klippel, A.; Kraus, M.; Bobkova, E. V.; Deshmukh, S.; Xu, Z.; Mueller, U.; Szwczak, A. A.; Pan, B. S.; Richon, V.; Pollock, R.; Blume-Jensen, P.; Northrup, A.; Andersen, J. N. Genetic and pharmacological inhibition of PDK1 in cancer cells: characterization of a selective allosteric kinase inhibitor. *J. Biol. Chem.* **2011**, *286*, 6433–6448.
- (73) Azam, M.; Seeliger, M. A.; Gray, N. S.; Kuriyan, J.; Daley, G. Q. Activation of tyrosine kinases by mutation of the gatekeeper threonine. *Nat. Struct. Mol. Biol.* **2008**, *15*, 1109–1118.
- (74) Baldwin, I.; Bamborough, P.; Haslam, C. G.; Hunjan, S. S.; Longstaff, T.; Mooney, C. J.; Patel, S.; Quinn, J.; Somers, D. O. Kinase array design, back to front: biaryl amides. *Bioorg. Med. Chem. Lett.* **2008**, *18*, 5285–5289.
- (75) DiMauro, E. F.; Newcomb, J.; Nunes, J. J.; Bemis, J. E.; Boucher, C.; Buchanan, J. L.; Buckner, W. H.; Cee, V. J.; Chai, L.; Deak, H. L.; Epstein, L. F.; Faust, T.; Gallant, P.; Geuns-Meyer, S. D.; Gore, A.; Gu, Y.; Henkle, B.; Hodous, B. L.; Hsieh, F.; Huang, X.; Kim, J. L.; Lee, J. H.; Martin, M. W.; Masse, C. E.; McGowan, D. C.; Metz, D.; Mohn, D.; Morgenstern, K. A.; Oliveira-dos-Santos, A.; Patel, V. F.; Powers, D.; Rose, P. E.; Schneider, S.; Tomlinson, S. A.; Tudor, Y. Y.; Turci, S. M.; Welcher, A. A.; White, R. D.; Zhao, H.; Zhu, L.; Zhu, X. Discovery of aminoquinazolines as potent, orally bioavailable inhibitors of Lck: synthesis, SAR, and in vivo anti-inflammatory activity. *J. Med. Chem.* **2006**, *49*, 5671–5686.
- (76) Patnaik, S.; Stevens, K. L.; Gerding, R.; Deanda, F.; Shotwell, J. B.; Tang, J.; Hamajima, T.; Nakamura, H.; Leesnitzer, M. A.; Hassell, A. M.; Shewchuck, L. M.; Kumar, R.; Lei, H.; Chamberlain, S. D. Discovery of 3,5-disubstituted-1*H*-pyrrolo[2,3-*b*]pyridines as potent inhibitors of the insulin-like growth factor-1 receptor (IGF-1R) tyrosine kinase. *Bioorg. Med. Chem. Lett.* **2009**, *19*, 3136–3140.
- (77) Cai, Z. W.; Wei, D.; Schroeder, G. M.; Cornelius, L. A.; Kim, K.; Chen, X. T.; Schmidt, R. J.; Williams, D. K.; Tokarski, J. S.; An, Y.; Sack, J. S.; Manne, V.; Kamath, A.; Zhang, Y.; Marathe, P.; Hunt, J. T.; Lombardo, L. J.; Fargnoli, J.; Borzilleri, R. M. Discovery of orally active pyrrolopyridine- and aminopyridine-based Met kinase inhibitors. *Bioorg. Med. Chem. Lett.* **2008**, *18*, 3224–3229.
- (78) Hodous, B. L.; Geuns-Meyer, S. D.; Hughes, P. E.; Albrecht, B. K.; Bellon, S.; Bready, J.; Caenepeel, S.; Cee, V. J.; Chaffee, S. C.; Coxon, A.; Emery, M.; Fretland, J.; Gallant, P.; Gu, Y.; Hoffman, D.; Johnson, R. E.; Kendall, R.; Kim, J. L.; Long, A. M.; Morrison, M.; Olivieri, P. R.; Patel, V. F.; Polverino, A.; Rose, P.; Tempest, P.; Wang, L.; Whittington, D. A.; Zhao, H. Evolution of a highly selective and potent 2-(pyridin-2-yl)-1,3,5-triazine Tie-2 kinase inhibitor. *J. Med. Chem.* **2007**, *50*, 611–626.
- (79) Hasegawa, M.; Nishigaki, N.; Washio, Y.; Kano, K.; Harris, P. A.; Sato, H.; Mori, I.; West, R. I.; Shibahara, M.; Toyoda, H.; Wang, L.; Nolte, R. T.; Veal, J. M.; Cheung, M. Discovery of novel benzimidazoles as potent inhibitors of TIE-2 and VEGFR-2 tyrosine kinase receptors. *J. Med. Chem.* **2007**, *50*, 4453–4470.
- (80) Aronov, A. M.; McClain, B.; Moody, C. S.; Murcko, M. A. Kinase-likeness and kinase-privileged fragments: toward virtual polypharmacology. *J. Med. Chem.* **2008**, *51*, 1214–1222.
- (81) Schulz, M. N.; Fanghanel, J.; Schafer, M.; Badock, V.; Briem, H.; Boemer, U.; Nguyen, D.; Husemann, M.; Hillig, R. C. A crystallographic fragment screen identifies cinnamic acid derivatives as starting points for potent Pim-1 inhibitors. *Acta Crystallogr.* **2011**, *D67*, 156–166.
- (82) Giordanetto, F.; Kull, B.; Dellsen, A. Discovery of novel class 1 phosphatidylinositol 3-kinases (PI3K) fragment inhibitors through structure-based virtual screening. *Bioorg. Med. Chem. Lett.* **2011**, *21*, 829–835.
- (83) Miller, D. D.; Bamborough, P.; Christopher, J. A.; Baldwin, I. R.; Champigny, A.; Cutler, G. J.; Kerns, J. K.; Longstaff, T.; Mellor, G. W.; Morey, J. V.; Morse, M. A.; Nie, H.; Taggart, J. J.; Rumsey, W. 3,5-Disubstituted-indole-7-carboxamides: the discovery of a novel series of potent, selective inhibitors of IKK- $\beta$ . *Bioorg. Med. Chem. Lett.* **2011**, *21*, 2255–2258.
- (84) Nadin, A.; Churcher, I. Manuscript in preparation.
- (85) Congreve, M.; Carr, R.; Murray, C.; Jhoti, H. A “rule of three” for fragment-based lead discovery? *Drug Discovery Today* **2003**, *8*, 876–877.
- (86) *Daylight Theory Manual*; Daylight Chemical Systems Inc.: Laguna Niguel, CA, 2008; <http://www.daylight.com/dayhtml/doc/theory/index.html>.
- (87) *LIGPREP*; Schrodinger Inc., 2010; <http://www.schrodinger.com>.
- (88) Cheeseright, T. J.; Mamat, B.; Melville, J. L.; Vinter, J. G. FieldScreen: virtual screening using molecular fields. Application to the DUD data set. *J. Chem. Inf. Model.* **2008**, *48*, 2108–2117.
- (89) Davies, D. R.; Mamat, B.; Magnusson, O. T.; Christensen, J.; Haraldsson, M. H.; Mishra, R.; Pease, B.; Hansen, E.; Singh, J.; Zembower, D.; Kim, H.; Kiselyov, A. S.; Burgin, A. B.; Gurney, M. E.; Stewart, L. J. *J. Med. Chem.* **2009**, *52*, 4694–4715.

## NOTE ADDED IN PROOF

Fragment 5 also inhibits leukotriene A4 hydrolase.<sup>89</sup>